5-2016

The Synthesis of Serine Competitive Inhibitors to Limit the Impact of Fungal Endocarditis

Michael R. Brouner
jvw515@vols.utk.edu

The Synthesis of Serine Competitive Inhibitors to Limit the Impact of Fungal Endocarditis

Honors Thesis Project

Chemistry Department

Dr. Michael Best's Research Lab

University of Tennessee, Knoxville

Michael Robert Brouner

May 2016

Table of Contents

Abstract

The overall purpose of this project is to successfully synthesize multiple analogs of L-serine that can act as competitive inhibitors of phosphatidylserine synthase from the fungal species *Candida albicans* and ultimately serve to provide vital information regarding the potential development of anti-fungal therapeutics against the fungal infection Fungal Endocarditis. The focus of this project centers around the necessity to determine a process by which researchers can synthesize a pharmaceutical drug that can put an end to the harmful impact of fungal infections within immunocompromised individuals. Biofilm formation on prosthetic heart valves leads to Fungal Endocarditis, which more often than not results in death for the infected individuals. The hope, by focusing on the differences in biochemical pathways between *C. albicans* and affected humans, is to discover a drug that can effectively render the functioning of *C. albicans* cells useless. While *C. albicans* requires the use of phosphatidylserine synthase to create phosphatidylserine, the biochemical pathway within humans follows an entirely different route. This difference in biochemical pathways between *C. albicans* and humans is a focal point of this research and provides a possible road for intervention of the adverse effects of *C. albicans* against humans. By competitively inhibiting phosphatidylserine synthase, the virulence of *C. albicans* is eradicated while mammals are not negatively affected. The compounds being synthesized for competitive inhibition testing are (*S*)-3-bromo-*N*-(1-carboxy-2-hydroxyethyl)propan-1-aminium, (*S*)-3-azido-*N*-(1-carboxy-2-hydroxyethyl)propan-1-aminium, and (*S*)-*N*-(1-carboxy-2-hydroxyethyl)prop-2-yn-1-aminium.

Compounds Utilized and Synthesized

L-serine	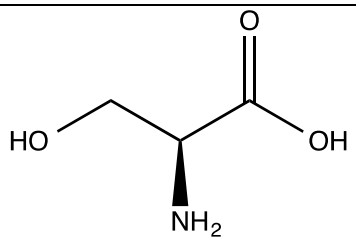
tert-butyl *O*-(*tert*-butyl)-*L*-serinate hydrochloride (**1**)	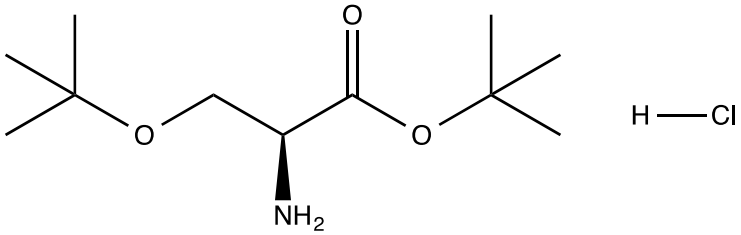
tert-butyl *O*-(*tert*-butyl)-*L*-serinate (**2**)	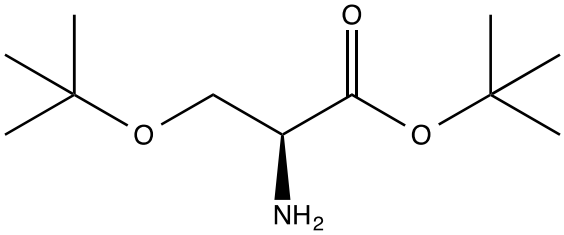
1,3-dibromopropane (**3**)	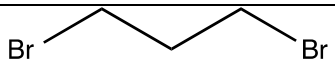
1-azido-3-bromopropane (**4**)	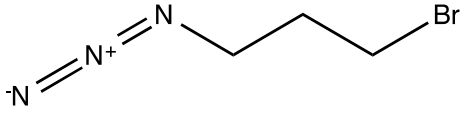
3-bromo-1-propyne (**5**)	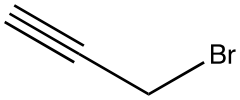

(*S*)-3-bromo-*N*-(1-carboxy-2-hydroxyethyl)propan-1-aminium (**6**)	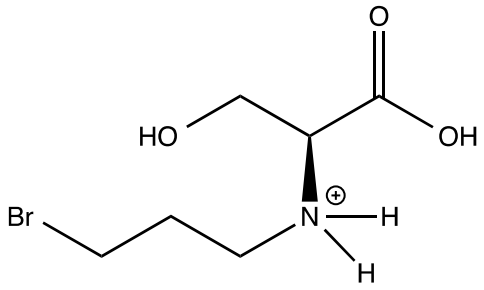
(*S*)-3-azido-*N*-(1-carboxy-2-hydroxyethyl)propan-1-aminium (**7**)	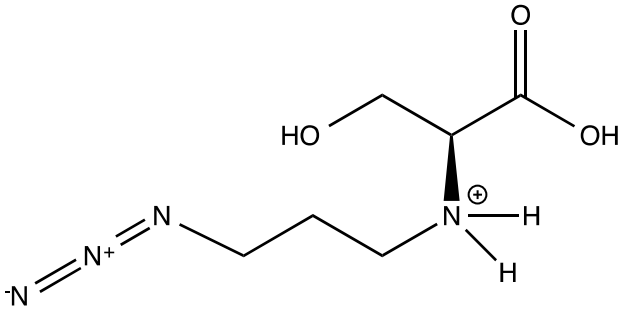
(*S*)-*N*-(1-carboxy-2-hydroxyethyl)prop-2-yn-1-aminium (**8**)	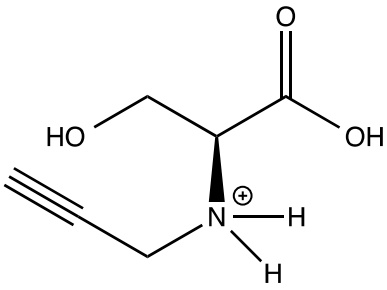

Introduction and Background

Fungal Endocarditis is one of the most prominent fungal infections still prevalent today that, regardless of the treatment methods used, has led to a high mortality rate, especially towards individuals who possess weaker immune systems (Mishra et al., 2007). Searches for a new type of drug to slow down the effects of Fungal Endocarditis is a necessity.

Fungal Endocarditis tends to appear in higher frequency in individuals who have cardiovascular systems that have undergone numerous surgical operations or in individuals who were born with abnormal hearts. Normally, one's innate defense systems prove sturdy enough to hold off the invasion of the fungal species into the heart altogether. In individuals with impaired defense systems, however, the fungal species manages to invade the heart through transportation within the blood stream.[9] The human heart can pump blood at an incredibly fast rate; some fungal invasions are thwarted immediately if the fungal species is not able to establish its presence fast enough before the incoming blood supply is pumped out of the aorta towards the rest of the body. If the fungal species is able to establish its presence within the innermost layer of tissue within the heart, the endocardium, the fungal species can then grow within the heart and lead to complications for the affected individual.

The complications that can plague an affected individual are numerous. Although the effects can range dramatically, the individuals affected tend to remain fairly constant: as one's heart strength and condition declines, one becomes more susceptible to the fungal infection Fungal Endocarditis. Congestive heart failure and possessing a prosthetic heart valve, for example, tend to increase one's chance of infection. Regardless of the reason why an individual may become infected, the outcome of infection is dismal. In a case study of 70 infected

individuals between 2000 and 2010, the average survival rate after 1 year of infection was only 41%.[1]

The fungal species that has been determined to be the initiator of the majority of Fungal Endocarditis cases is *C. albicans*.[8] The majority of these infections are caused by the biofilm formation of *C. albicans* on implanted cardiac devices such as prosthetic heart valves, indwelling catheters, and pacemakers.[5] The effects of *C. albicans* are not solely limited to the cardiovascular system; *C. albicans* has been shown to play a role in multiple oral cavity diseases, including chronic periodontitis, dental caries, and angular cheilitis.[7]

Biofilm formation is prefaced by an organism's attachment to a surface and production of extracellular polysaccharides.[4] Once the organism is able to establish its presence and then replicate, the biofilm growth gradually increases in a rate corresponding to the collective rate of replication of all organisms within the biofilm. For the *Candida* species, biofilm formation involves the "matrix-enclosed microcolonies of yeasts and hyphae, arranged in a bilayer structure."[5] After a biofilm has formed and spread to a significant size, it begins behaving as a colony of organisms that group together. Individual organisms within a biofilm can communicate with one another and fight off complete eradication more easily than an isolated individual organism is able to do alone. If a synthesized drug were able to eradicate the wild type species of *C. albicans,* the individual fungal organisms would likely die prior to replication. In a biofilm, however, the odds of one of the organisms possessing a beneficial mutation are likely. It is very possible that a synthesized drug would be ineffective against a biofilm because if one of the organisms can manage to survive and replicate, resistance is conferred to the biofilm. Thus, survival and replication is more likely for a biofilm than for isolated organisms.

The first step in attempting to prohibit the negative effects of a biofilm created by *C. albicans* is to stop or slow down the formation of the biofilm altogether. The goal of this project is to synthesize a compound that can serve as a competitive inhibitor in a key biochemical reaction present within *C. albicans* but not within mammals. Specifically, the goal of this research is to find a suitable way to inhibit the production of phosphatidylserine within *C. albicans* without affecting biochemical reactions within mammals along the way.

Competitive inhibitors have the ability to reduce the binding of substrates to its desired enzyme, effectively limiting the enzyme activity. Competitive inhibitors bind to the same enzyme that substrates naturally bind to, thus creating a competition between the inhibitors and the substrate. To synthesize a suitable competitive inhibitor, the inhibitor needs to mimic the binding characteristics of the substrate's binding site. In effect, the inhibitor needs to serve the purpose of being a "clone" of the substrate, effectively reducing the amount of binding the substrate can have with respect to the desired enzyme.

The targeted enzyme of choice present within *C. albicans* is the specific phosphatidylserine synthase, Cho1. Cho1 is a great target enzyme for a competitive inhibitor for two main reasons: 1. The synthesis of phospholipids in *C. albicans,* which involves the use of phosphatidylserine synthase, follows a different pathway than the phospholipid synthesis within mammals, which does not require phosphatidylserine synthase for phospholipid synthesis.[2] 2. The substrate that attaches to phosphatidylserine synthase is serine, which is a relatively simple molecule to slightly alter while keeping its core backbone intact.

The effect of inhibition of phosphatidylserine synthase studied in mouse models has shown a decrease in the amount of phosphatidylserine produced. As the production of

phosphatidylserine declines, the amount of masking of cell wall beta (1-3)-glucan is subsequently decreased as well.[3] As a result, host immunity stands a better chance to locate the invading fungal species and fight off the Fungal Endocarditis infection.

In general, a human's immune system is broken down into innate and adaptive divisions; the innate division is always active against infection while the adaptive immune system targets specific pathogens. Once an innate division cell spots an invader, it can signal to the adaptive immune system to help ward off the invading species. But what happens when the invader isn't spotted? This is why Fungal Endocarditis has grown to be such a major problem. Phosphatidylserine can help mask the beta(1,3)-glucan cell wall from the innate immune system. But once the masking of the cell wall is diminished, the fungal species can be spotted by the innate immune system and ultimately attacked and destroyed by the adaptive immune system. Causing a decrease in the production of phosphatidylserine, by competitive inhibition of phosphatidylserine synthase, can in turn lead to the spotting and destruction of invading fungal species that would otherwise lead to the fungal infection Fungal Endocarditis.

The desired final products within this research group will be analogs of L-serine that have the potential to bind to phosphatidylserine synthase and hopefully limit the growth and proliferation of *C. albicans* as a subsequent result.

The structure of serine contains four main substituents that extend from a central carbon atom. Three of the four substituents are consistent with all naturally occurring amino acids: a hydrogen atom, a carboxyl group, and an amino group. The fourth substituent, which distinguishes serine from other amino acids, is an R group that is represented by CH_2OH. Of the

twenty naturally occurring amino acids, serine is one of only five of the amino acids that are polar, with the other polar amino acids including asparagine, cysteine, glutamine, and threonine.

In a typical amino acid chain, a peptide bond is formed when the nitrogen atom contained within the amino substituent group on one amino acid attacks the carbon atom contained within the carboxyl substituent group of another amino acid, resulting in a loss of a water molecule. Within the research performed in this project, we want to emulate a similar attack by the amino substituent group, but in this instance, we wish to manipulate the nucleophilic nitrogen of the serine amino background into initiating a substitution reaction with 1,3 – dibromopropane (**3**), 1-azido-3-bromopropane (**4**), and 3-bromo-1-propyne (**5**) respectively in the hopes of obtaining serine analogs that are very similar, but still possess differences, with natural serine.

The starting material for our compound syntheses is *tert*-butyl *O*-(*tert*-butyl)-*L*-serinate hydrochloride (**1**) instead of natural serine. By utilizing Compound **1** instead of serine**,** we can manipulate the nucleophilic nitrogen of Compound **1** into initiating substitution reactions with 1,3 – dibromopropane (**3**), 1-azido-3-bromopropane (**4**), and 3-bromo-1-propyne (**5**) instead of intramolecularly interacting with the hydroxyl groups that would have been present within natural serine. Because the starting material has O-(tert-butyl) groups instead of OH groups, the nucleophilic nitrogen is unable to intramolecularly interact with the OH groups of natural serine. As a result, it is now possible to effectively vary the backbone of serine. After the substitution reaction is completed, a deprotection step removes the tert-butyl groups and the final synthesized compounds resemble natural serine, although their amino group backbones have been slightly altered.

To date, the serine analogs that have undergone substitution with 1-azido-3-bromopropane (**4**) and 3-bromo-1-propyne (**5**) have been tracked intracellularly by utilizing clickable tags. Through the use of the two clickable substrate analogs in a phosphatidylserine synthase assay performed by graduate student Chelsi Cassilly, it has been discovered that both analogs, Compound **7** and Compound **8,** compete with serine and effectively inhibit the production of phosphatidylserine. The third serine analog synthesized within this research group, Compound **6**, which involves the substitution of 1,3-dibromopropane (**3**), is hoped to be even more effective in causing competitive inhibition of Cho1.

While the relative inhibition effects of Compounds **7** and **8** are merely designed to discover more information about the binding site characteristics of Cho1, Compound **6** has the potential to make strong headway in the future design of a pharmaceutical drug to fight off a *C. albicans* infection. Compound **6**'s backbone possesses a bromine leaving group that is very prone to substitution reactions. If the binding site of Cho1 potentially were to initiate a substitution reaction with Compound **6**, the enzyme's binding site would be drastically altered. In essence, Compound **6** could potentially serve as an irreversible competitive inhibitor of Cho1 if the enzyme's binding site was rendered unable to bind serine after interacting with Compound **6**.

Figure 1 – Preliminary Inhibition Results for Compound **7**

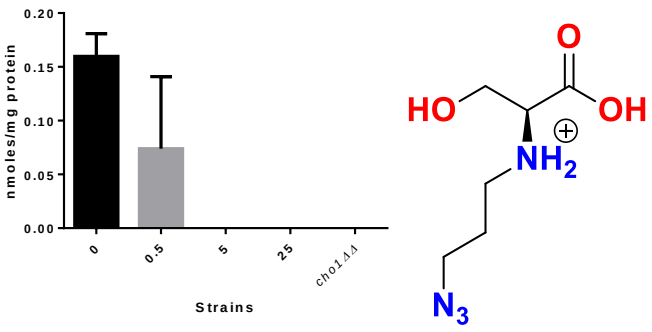

Based on the results from Figure 1, the phosphatidylserine synthase Chol within *C. albicans* in increasingly inhibited as the concentration of Compound **7** increases. When Compound **7** is not present, the formation of phosphatidylserine, as monitored by a scintillation counter, is approximately 16 nmol/mg protein. When only 0.5 mmol of Compound **7** is introduced, however, the production of phosphatidylserine decreases by over 50%. When 5 mmol of Compound **7** or more are introduced, the production of phosphatidylserine is completely diminished and it becomes increasingly suggestive that Compound **7** is a suitable competitive inhibitor of Cho1.

Figure 2 – Preliminary Inhibition Results for Compound **8**

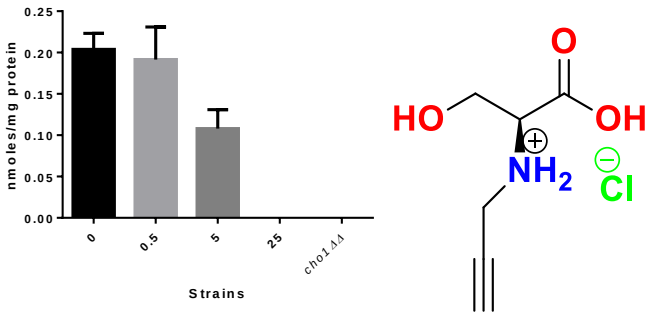

Based on the results from Figure 2, the phosphatidylserine synthase Cho1 within *C. albicans* is increasingly inhibited as the concentration of Compound **8** increases. When only 0.5 mmol of Compound **8** introduced, the reduction in production of phosphatidylserine is minimal. When 5 mmol of Compound **8** are introduced, however, the production of phosphatidylserine decreases by roughly 50%. With 25 mmol of Compound **8,** the production of phosphatidylserine is entirely diminished, again suggesting the successful inhibition of Cho1 by a synthesized compound made within this research group. It should be noted that standard error bar analysis of Figures 1 and 2 would suggest that the results obtained from Compound **8** are more reliable than the results obtained for Compound **7** at this time.

Synthesis Design

Figure 3 – Synthesis Scheme

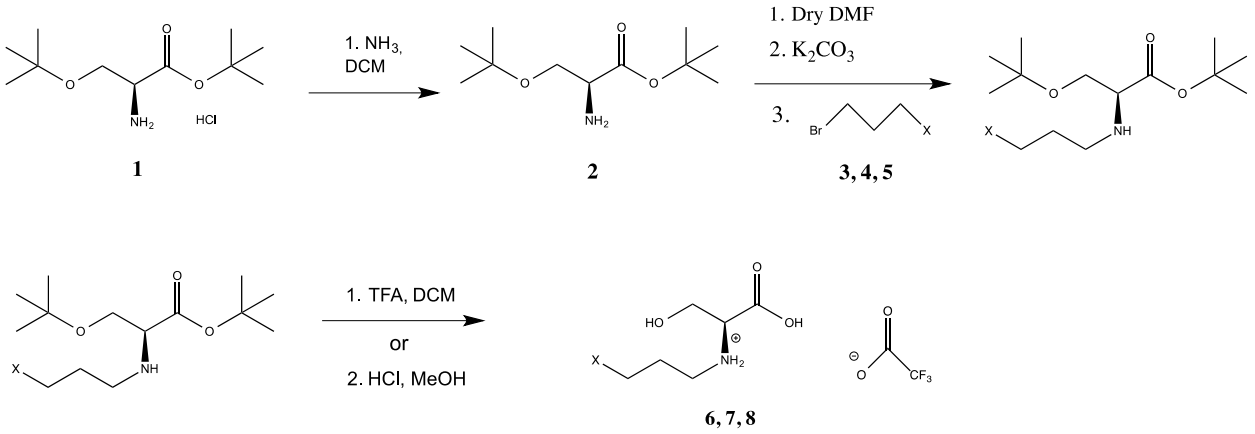

The above synthesis sequence portrayed by Figure 3 proceeds by means of three general reactions: respectively, extraction of HCl by use of NH_3, an Sn2 substitution reaction, and deprotection.

In the initial portion of Figure 3, the starting material **1** is a salt. The NH_2 portion of the starting material is a free base and will be protonated easily in the presence of acid. Because HCl, a strong acid, is present, the NH_2 portion of the starting material has been protonated to $^{+}NH_3$ and is a hydrochloric salt. In an attempt to form the basic NH_2 again, extraction with NH_3 helps remove HCl from the solution.

In the second portion of Figure 3, an S_N2 substitution reaction occurs that involves the nucleophilic attack of the nitrogen atom within NH_2 and the departure of the bromine leaving group on Compounds **3**, **4**, and **5**. The mechanism of the S_N2 substitution reaction can be seen in Figure 4 on the following page.

Figure 4 – S_N2 Substitution Reaction

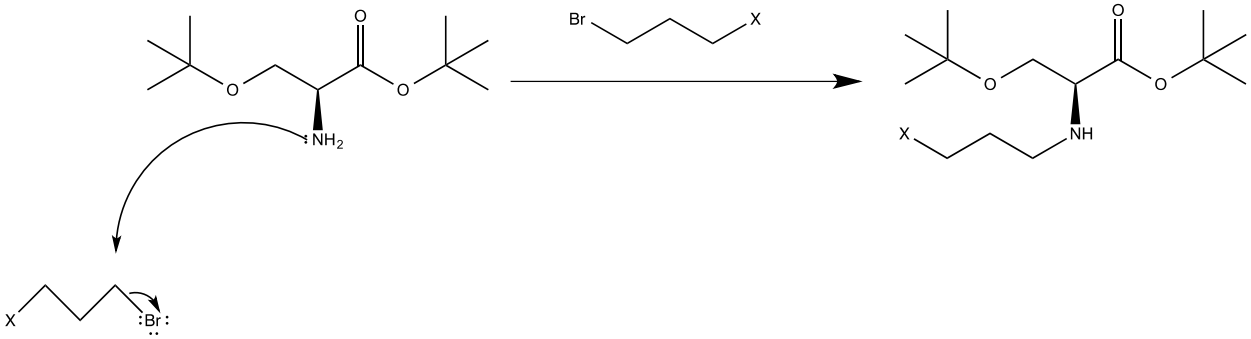

In the final portion of Figure 3, deprotection of the tert-butyl groups occurs with use of trifluoroacetic acid (TFA)[1]. The deprotection step involves the removal of both tert-butyl groups and replacement of hydrogen atoms in their place.

Figure 5 – Deprotection Step

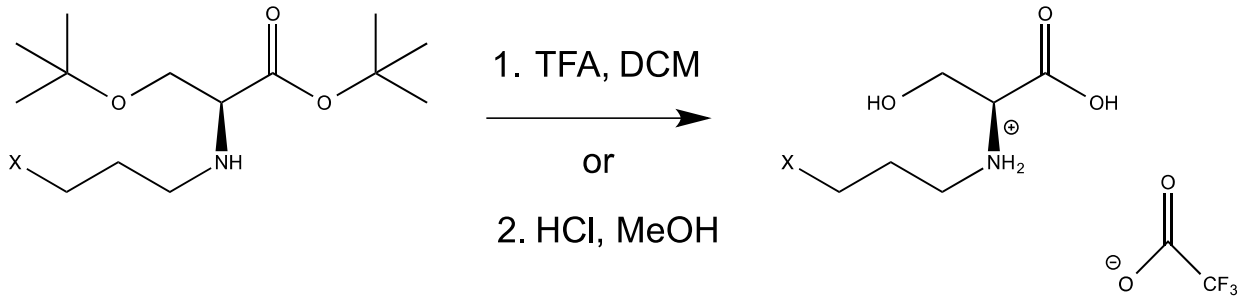

[1] Hydrochloric acid (HCl) in methanol (MeOH) was later utilized as a deprotecting group instead of TFA.

Experimental Procedure

In the overall reaction, the addition of Compounds **3**, **4**, and **5**, respectively 1,3 – dibromopropane, 1-azido-3-bromopropane, and 3-bromo-1-propyne, differentiated the various portions of the synthesis reactions. Regardless of which of the three compounds was utilized for each respective portion of the experiment, each of the general schemes followed the same general outline. The outline of the synthesis involved 5 distinct parts.

Part 1: The Extraction of *tert*-butyl *O*-(*tert*-butyl)-*L*-serinate hydrochloride (1) into *tert-butyl* O-(tert-butyl)-L-serinate (2)

First, Compound **1** (0.100 g) was weighed and subsequently transferred into a separatory funnel for extraction using ammonia (5%, 20 – 25 mL) and dichloromethane (80 mL). The funnel was stoppered and shaken 3 separate times, with the gaseous byproduct being allowed to exit the funnel after each individual shake by slightly opening the separatory funnel's valve with the valve oriented in an upward fashion. The bottom, organic layer of solution (the one containing the DCM) was collected into a clean 250-mL Erlenmeyer flask. The DCM was added 3 to 5 separate times until the resulting solution within the Erlenmeyer flask was approximately 100 mL. During each individual section of the extraction, the bottom (organic) layer was allowed to separate from the top (aqueous) layer prior to draining the organic layer through the bottom of the separatory funnel. In an effort to diminish the amount of aqueous contamination within the organic layer, the organic layer was filtered through the bottom of the separatory funnel instead of being poured out of the top of the separatory funnel (where the aqueous layer was residing).

Next, to remove the residual H_2O, a drying agent, anhydrous sodium sulfate, was utilized. The collected organic layer was then decanted into a clean, pre-weighed 250 mL round bottom flask, leaving the drying agent behind in the Erlenmeyer flask.

By utilizing a rotary evaporator, the solvent layer containing DCM within the round bottom flask was removed by rotating the rotary evaporator at a temperature of 55°C. After the rotary evaporator had removed nearly all, if not all, of the DCM layer, the round bottom flask was next placed on high vacuum overnight. The resulting product was Compound **2**.

Part 2: The Preparation of Compounds 3, 4, and 5

For the first portion of the experiment, 1,3 - dibromopropane (**3**) was already a reactant possessed within Dr. Best's laboratory. No further steps were required to prepare the desired haloalkane.

For the second portion of the experiment, 1-azido-3-bromopropane (**4**) was synthesized by reacting sodium azide (0.235 g, 3.6 mmol, 1.18 eq) with 1,3-dibromopropane (310 μL, 3.05 mmol, 1 eq) in a 250 mL round bottom flask that already contained acetonitrile (20-25 mL). A stir bar was added and the flask was then placed within an oil bath and refluxed overnight at 50°C with stirring. After refluxing and stirring overnight, the round bottom flask was removed from the oil. By utilizing deionized water (20 mL) and DCM (approximately 75 mL in total), an extraction was performed that collected the bottom organic layer in a clean Erlenmeyer flask. Sodium sulfate was used to remove any residual H_2O in the remaining solution within the Erlenmeyer flask. The solution was then transferred to a round bottom flask that was subsequently placed on the rotary evaporator to remove the DCM solvent in the solution. ^{1}H – Nuclear Magnetic Resonance (^{1}H-NMR) and mass spectrometry were utilized to determine if

Compound **4** had formed. The final product of this step was transferred, using copious amounts of DCM, into a clean vial and stoppered. The results of Compound **4**'s synthesis are portrayed in Figures 6 and 7 within the Results and Discussion section of this report.

For the third portion of the experiment, 3-bromo-1-propyne (**5**) was a compound already possessed within Dr. Best's laboratory.

Part 3: The Addition of Compounds 3, 4, and 5 to Compound 2

During this lengthier phase of the experiment, multiple steps were performed that attempted to first specifically add Compounds **3**, **4**, or **5** onto the nitrogen atom within Compound **2** then deprotect and subsequently remove the tert-butyl groups located on Compound **2** to reach the desired serine analog.

First, dry DMF (20 mL) was added to the round bottom flask containing Compound **2** (0.098 g, 0.451 mmol, 1 eq) retrieved from extraction in Part 1 of the experiment. Next, potassium carbonate (0.160 g, 1.16 mmol, 2.57 eq) was added to the flask and the solution was stirred for 20 minutes. Then, Compound **3** (60 μL, 0.59 mmol, 1.3 eq) was added to the solution within the round bottom flask using a pipet. The round bottom flask was then placed in an oil bath at 55° C and refluxed while stirring overnight.

The previous step described the procedure followed for the substitution reaction involving Compound **3** in the hope of creating Compound **6**. Similar workups were performed for Compounds **4** and **5** in the hopes of respectively creating Compounds **7** and **8** as well.

For the reaction to produce Compound **7**, Compound **2** (0.094 g, 0.433 mmol, 1 eq), potassium carbonate (0.150 g, 1.085 mmol, 2.5 eq), Compound **4** (0.085 g, 0.52 mmol, 1.2 eq), and dry DMF (20 mL) were utilized.

For the reaction to produce Compound **8**, Compound **2** (0.200 g, 0.920 mmol, 1 eq), potassium carbonate (0.318 g, 2.30 mmol, 2.5 eq), Compound **5** (0.1053 mL, 1.18 mmol, 1.28 eq), and dry DMF (20 mL) were utilized. The synthesis of Compound **8** was performed by graduate student Shahrina Alam.

The reflux reaction was stopped after 24 hours. The next addition to the round bottom flask included copious amounts of ice with cold deionized water. The solution within the round bottom flask was placed into a separatory funnel and extracted using DCM (75 mL). The bottom, organic layer was collected in an Erlenmeyer flask and was dried over sodium sulfate. The solution was decanted into a clean 250 mL round bottom flask and placed on the rotary evaporator at approximately 85° C.

Next, the resulting solution was purified by utilizing column chromatography with an eluent of 25% ethyl acetate in hexane. Fractioning columns were utilized to help isolate specific solutions during the course of the synthesis reaction. The fractions collected were placed within test tubes and allowed to sit undisturbed for at least 12 hours to allow for the product to become better concentrated.

The test tubes were then separately spotted onto TLC plates. The TLC plates were in turn run through a TLC chamber containing 35% ethyl acetate – 65% hexane, observed under UV light, and then reacted with ninhydrin, potassium permanganate, and potassium permanganate respectively for the intermediates formed by addition of Compounds **3**, **4**, and **5**. The prominent spots that were portrayed by the TLC plates represented the fractions that potentially contained the desired product. The corresponding test tubes for the positive fractions were collected, rinsed

with DCM, and transferred into a round bottom flask that was placed on the rotary evaporator at 55° Celsius.

Next, trifluoroacetic acid (TFA) in a solvent of DCM was utilized to deprotect the tert-butyl groups located on the ends of Compound **2**. In latter stages of the experiment, HCl was substituted in the place of TFA as a deprotecting agent with methanol used as a solvent instead of DCM. Prior to the addition of TFA, DCM (15 mL) was added to the round bottom flask containing the desired intermediate. Then, TFA (8 mL) was added to the round bottom flask drop-wise and the solution was stirred overnight. After 24 hours, DCM was placed in the round bottom flask to assist the evaporation of TFA by the rotary evaporator. The solution was placed on the rotary evaporator 3 separate times after placing DCM into the round bottom flask before each respective solvent evaporation. After all of the TFA had evaporated, the solution was placed on high vacuum to ensure that all surrounding solvent had been successfully removed prior to proceeding with the next phase of Part 3.

To further purify the intermediate, reverse phase column chromatography was performed. The preconditioning of the reverse phase column included the following steps: 10 mL of 100% methanol; 8 mL of methanol and 2 mL of water; 6 mL of methanol and 4 mL of water; 4 mL of methanol and 6 mL of water; 2 mL of methanol and 8 mL of water; 10 mL of water. After each separate precondition was run through the column, the intermediate was then added to the reverse phase column using a pipet to transfer the solution. Each of the following "additions" were placed within the round bottom flask containing the intermediate and pipetted into the column from the flask, dragging along the intermediate gradually with them: 10 mL of 100% water; 8 mL of water and 2 mL of methanol; 6 mL of water and 4 mL of methanol; 4 mL of water and 6 mL of methanol; 2 mL of water and 8 mL of methanol; 10 mL of methanol.

The reverse phase column yielded a range of 10 - 12 test tubes. TLC analysis was then performed to determine the fractions that likely possessed the desired final compound. The fractions corresponding to the prominent spots observed after staining with ninhydrin during TLC analysis were then rinsed thoroughly with methanol, transferred to a round bottom flask, and again placed on the rotary evaporator. After rotary evaporation, the final compounds present within the round bottom flask were either Compound **6**, **7**, or **8**. To confirm the presence of the final products, NMR and mass spectrometry analysis were utilized.

Results and Discussion

There were a total of four different compounds produced – one intermediate (**4**) and three final products (**6**, **7**, and **8**). Both ^{1}H-NMR and ^{13}C-NMR were taken on a 500 MHz NMR spectrometer and mass spectrometry results were obtained by use of DART-TOF. For the intermediate formed in Part 2 of the Experimental Procedure, 1 – azido – 3 – bromopropane (**4**), ^{1}H-NMR and mass spectrometry were performed to analyze the potential formation of the desired intermediate. The results from ^{1}H-NMR and mass spectrometry for Compound **4** can be viewed in Figures 6 and 7 respectively.

Figure 6 – ^{1}H-NMR Results for Compound **4**

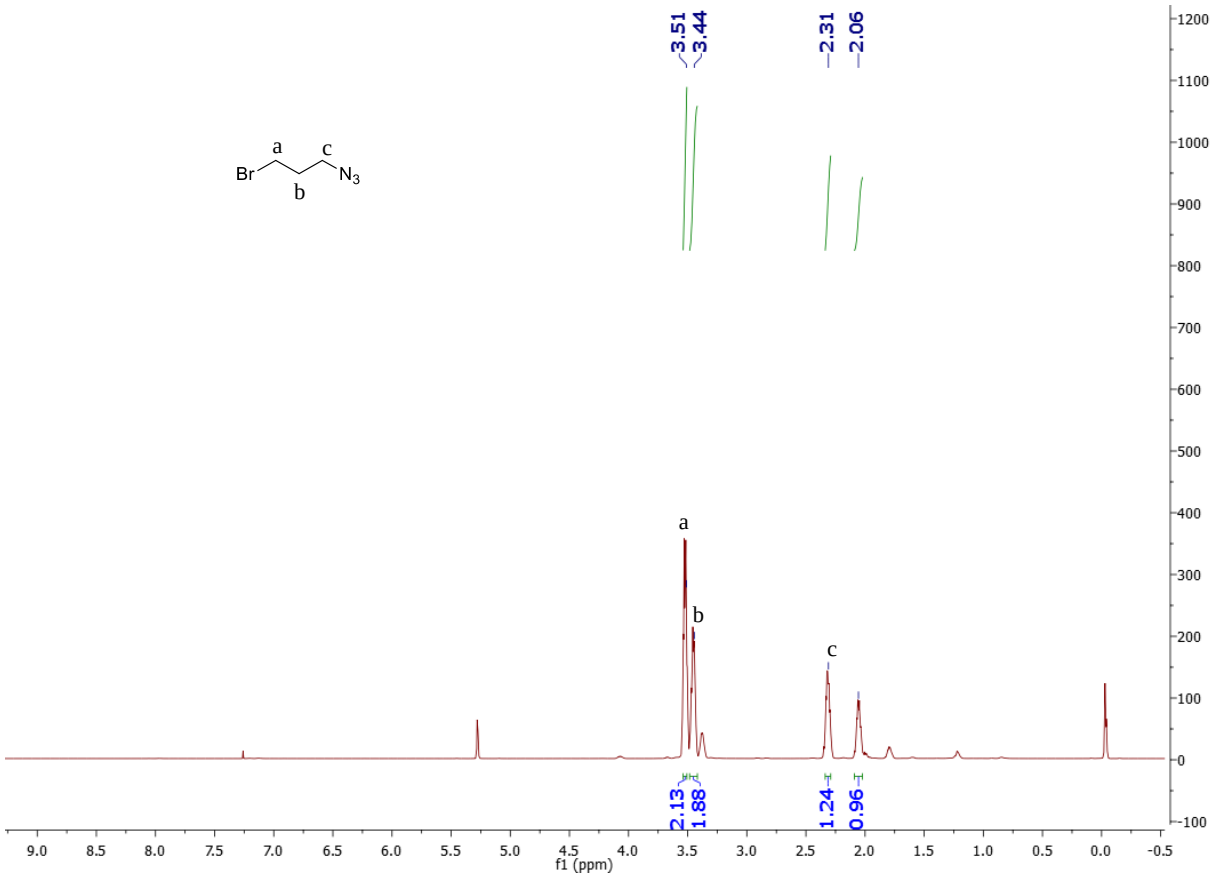

There are a total of 6 hydrogen atoms present within 1-azido-3-bromopropane (**4**) and one should expect ^{1}H-NMR data to portray integrated peaks equal to approximately 6. One should also expect that the peak representing the hydrogen atoms located nearest the bromine atom should be shifted further downfield than the peak representing the hydrogen atoms located on the carbon atom nearest the N_3 group. These expectations are due to bromine's high electronegativity leading to a shift further downfield for hydrogen atoms near the bromine molecule.

The ^{1}H-NMR data collected match the expected results. There were separate peaks at 3.54 ppm and 2.30 ppm, represented by letters a and c, that corresponded to the hydrogen atoms nearest the bromine atom and azide group respectively. In addition, the total integrated values of the peaks within the spectrum summed to 6.21, suggesting the presence of 6 hydrogen atoms within Compound **4** as anticipated.

Figure 7 – Mass Spectrometry for Compound **4**

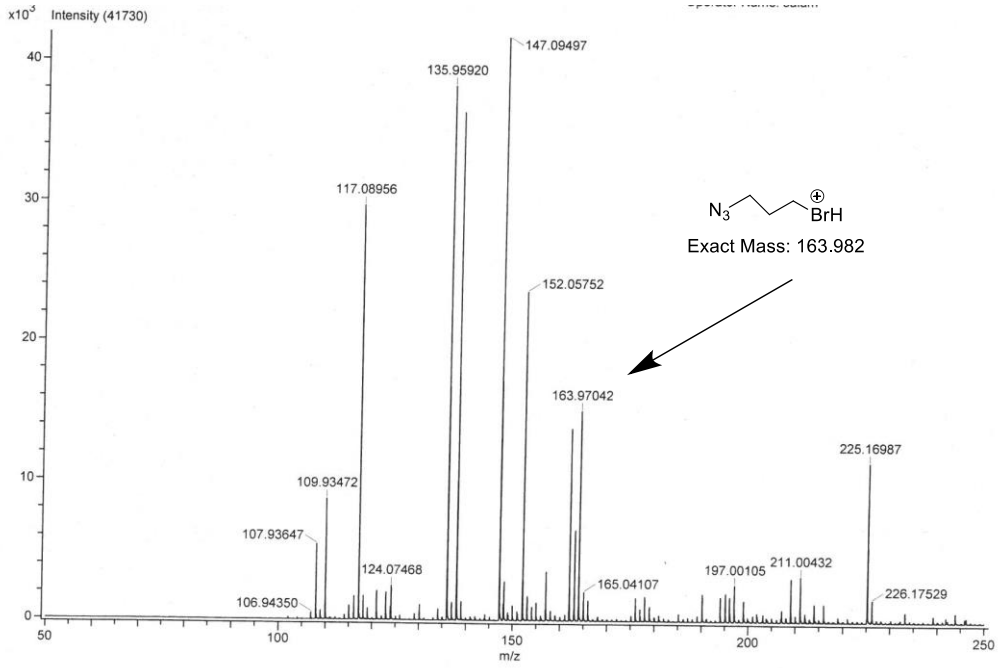

The exact mass of the molecular ion of Compound **4** is 163.982 m/z. The observed molecular ion from mass spectrometry was 163.97042 m/z as portrayed in Figure 7, containing a percent error of only 0.0000706 % (70.6 ppm).

To determine if the formation of (*S*)-3-bromo-*N*-(1-carboxy-2-hydroxyethyl)propan-1-aminium (**6**) occurred properly, ^{1}H-NMR, ^{13}C-NMR, and mass spectrometry were analyzed. The results are shown in Figures 8, 9, and 10 respectively.

Figure 8 – ^{1}H NMR for Compound **6**

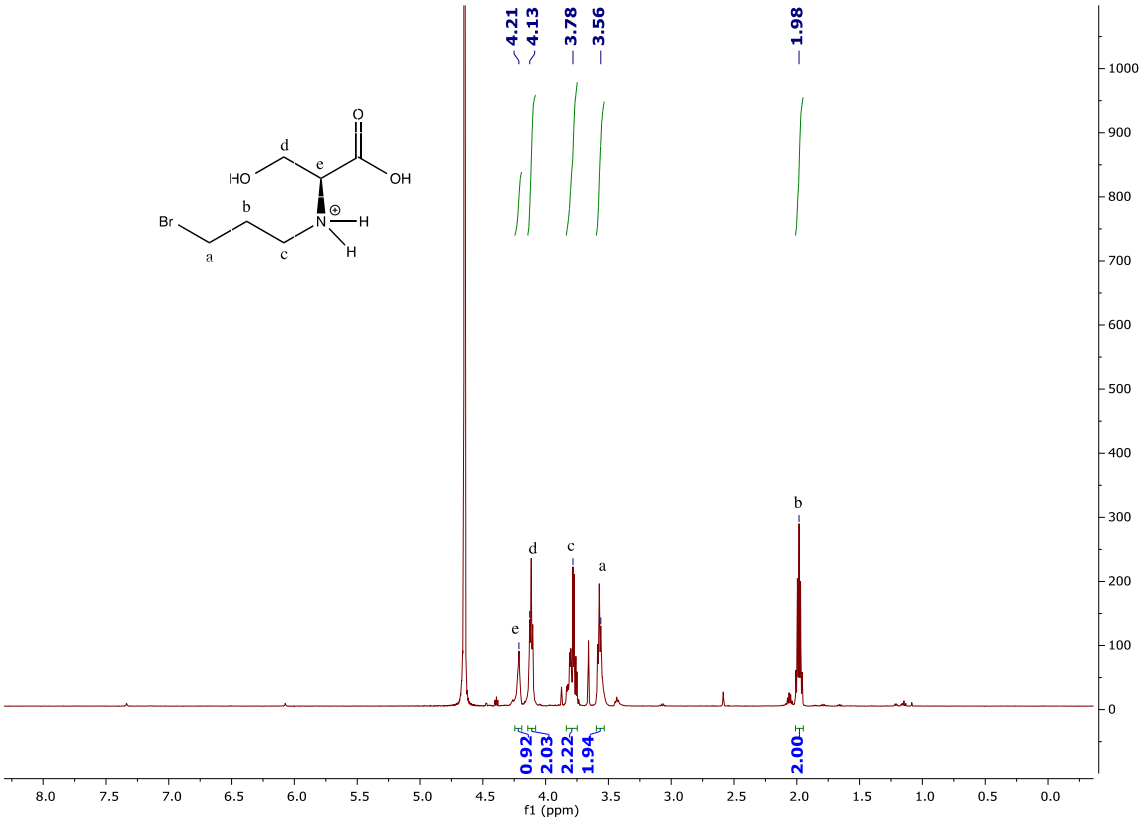

The hydrogen atoms present on the hydroxyl –OH, carboxylic acid –COOH, and the amine –NH_2 were shifted much further downfield than the area of interest within the ^{1}H-NMR spectra and will not be discussed during analysis. For the remaining 9 hydrogen atoms, it was

expected for the ^{1}H-NMR spectrum to portray 5 distinct peaks corresponding to the 5 distinct hydrogen atoms (or equivalent hydrogen atoms). Additionally, it was anticipated for one of the integrated peaks to sum to 1 in representation of Letter e, which only possesses 1 hydrogen atom.

The spectrum matched the expected results. Each distinct hydrogen atom, or set of equivalent hydrogen atoms, was represented by a distinct peak within the spectrum as hoped. Letters a, b, c, and d each possessed 2 equivalent hydrogen atoms and integrated to 1.94, 2.00, 2.22, and 2.03 respectively. Letter e possessed 1 hydrogen atom and integrated to 0.92. Letter b's peak was shifted most upfield in comparison to the rest of the peaks because of its isolation from all electron-withdrawing groups present within Compound **6**.

Figure 9 – ^{13}C-NMR for Compound **6**

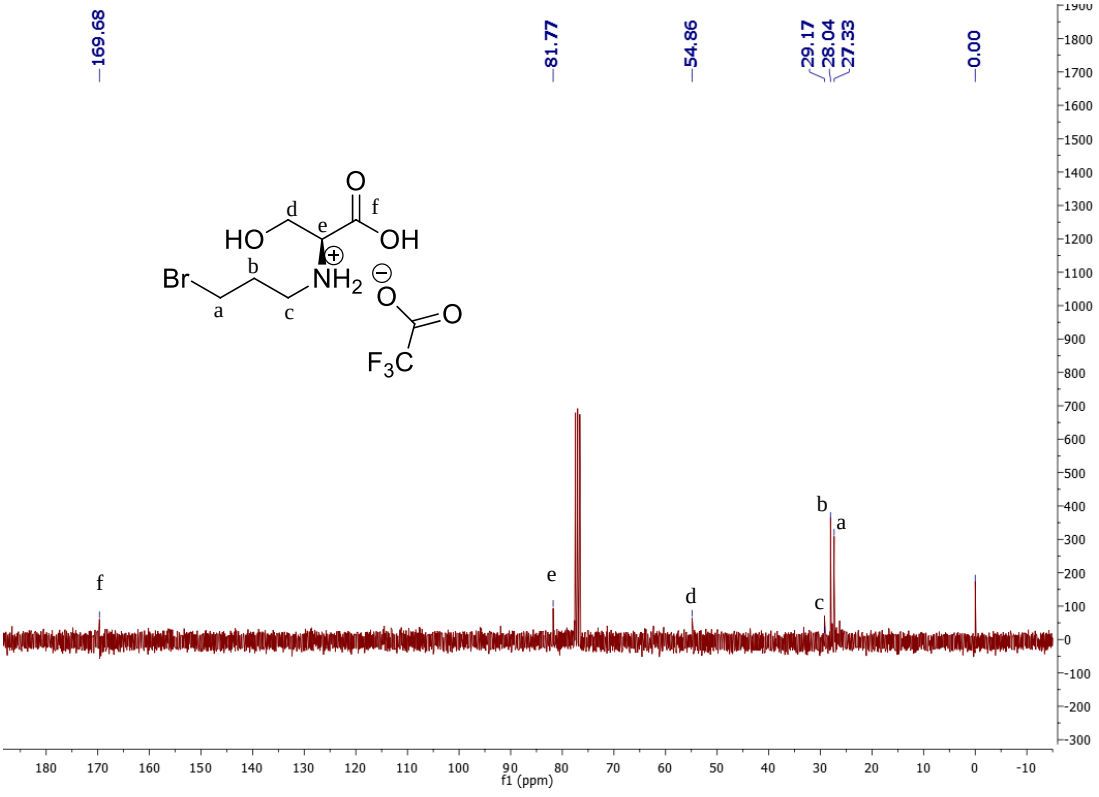

It was initially expected that the carbon atoms represented by letters c and d would both have been shifted further downfield. Based on the ^{13}C-NMR, it is very likely that there are impurities present within the desired final compound.

Figure 10 – Mass Spectrometry for Compound **6**

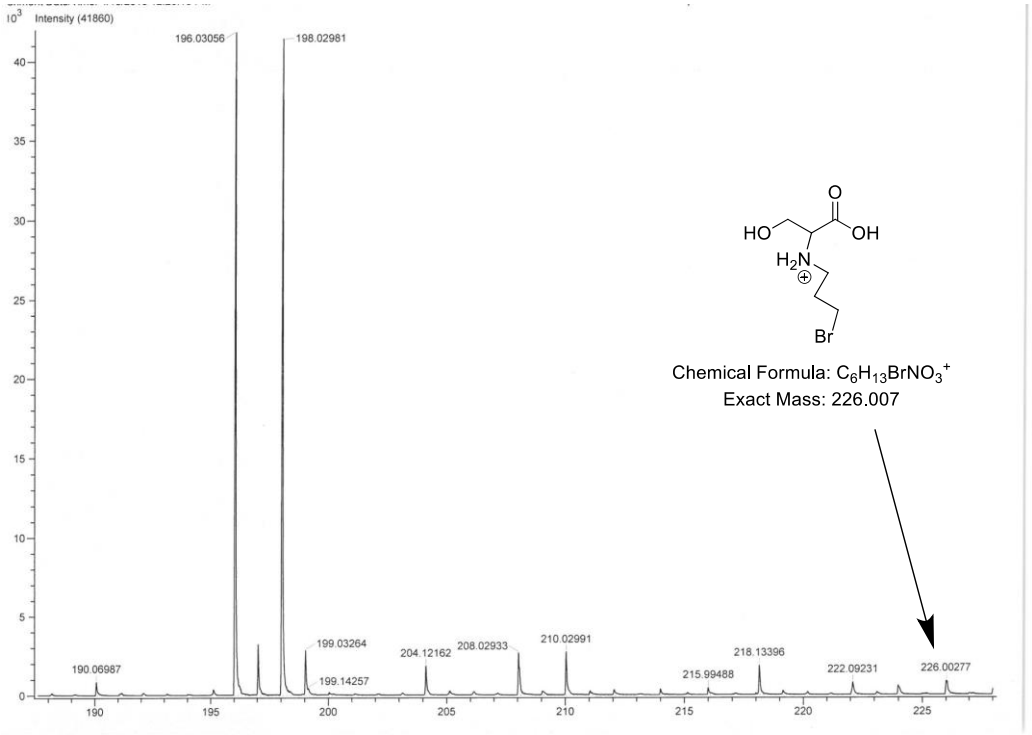

Mass spectrometry will produce fragments of an initial molecule that possess differing molecular weights relative to the portions of the initial molecule that still remain. In the case of Compound **6**, it was not entirely certain whether the final compound would possess a cyclic or acyclic structure initially. If Compound **6** were cyclic, it would be expected for its molecular weight prior to fragmentation to be near its exact mass of 146.081 m/z. If Compound **6** were acyclic, it would be expected for its molecular ion before fragmentation to be near its exact mass of 226.007 m/z. Mass spectrometry results strongly suggests Compound **6** is acyclic, as its

molecular ion's weight is equal to 226.00277 m/z and has a percent error of 0.0000187 % (18.7 ppm). In further support of that claim, TLC results obtained as detailed in the Experimental Procedure provided further evidence of the formation of the acyclic final product. Ninhydrin will only show positive spotting for primary and secondary amines but will not show spotting for any tertiary amines. If Compound **6** were cyclic, and subsequently possessed a tertiary amine within its structure, ninhydrin would not be expected to produce any positive spots. But ninhydrin was found to produce positive spotting for Compound **6**, strongly suggesting that Compound **6** is acyclic and not cyclic.

To determine if the synthesis of Compound **7** was successful, mass spectrometry and ^{1}H-NMR were analyzed. The results are shown in Figures 11 and 12, respectively.

Figure 11 – Mass Spectrometry for Compound **7**

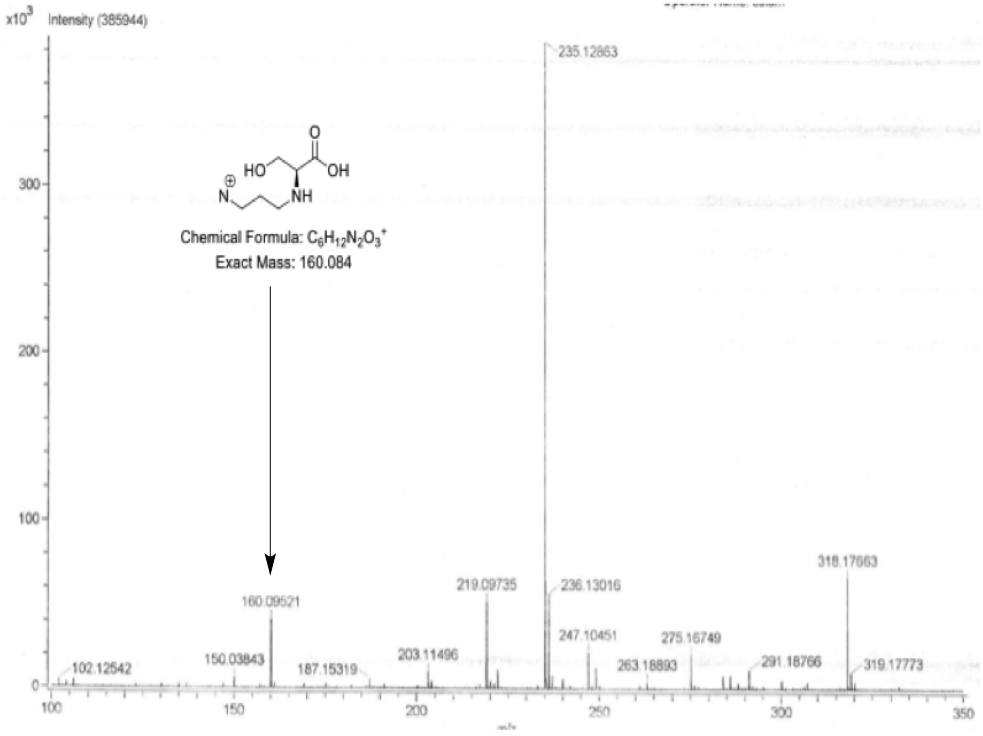

Compound **7**'s molecular weight after the loss of two nitrogen atoms is exactly 160.084 m/z. The mass spectrometry results obtained for the same molecular fragment of Compound **7** portrayed a molecular weight of 160.09521 m/z. The percent error associated with the molecular fragment's weight determination was 0.000070 % (70.0 ppm). Although this cannot entirely confirm the presence of Compound **7**, it strongly suggests that the synthesis occurred as hoped.

Figure 12 – ^{1}H-NMR for Compound **7**

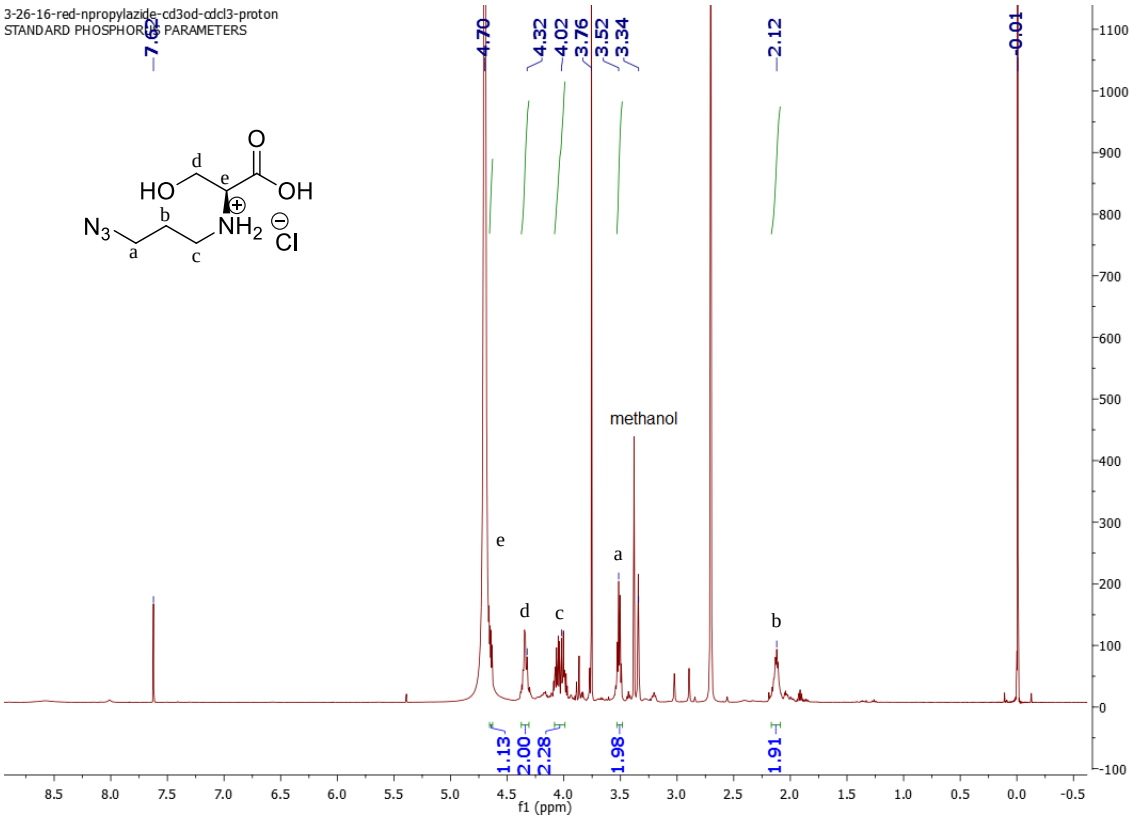

The ^{1}H-NMR spectrum obtained suggests the successful formation of Compound **7.** The peaks representing the hydrogen atoms located on Letters a, b, c, and d each had an integration of approximately 2 as expected. Letter e, which represents a single hydrogen atom, integrated as expected to 1.13 (approximately 1). Additionally, Letter b, which is shifted further upfield because of its isolation from electron withdrawing groups, correctly is portrayed by a multiplet in

the NMR spectrum, suggesting that its neighboring carbon atoms possess multiple hydrogen atoms (the neighboring carbon atoms possess a combined 4 hydrogen atoms). Letter a, which is slightly further downfield than Letter b, is correctly portrayed as a triplet in the NMR spectrum, as its neighboring carbon atom possesses 2 hydrogen atoms.

Furthermore, the peaks shifted further downfield represented Letters d and e, the two sets of hydrogen atoms nearest the hydroxyl group and carboxylic acid group respectively as anticipated.

To analyze the potential formation of Compound **8**, ^{1}H-NMR, ^{13}C-NMR, and mass spectrometry data were analyzed. The results are portrayed in Figures 13, 14, and 15 respectively.

Figure 13 – ^{1}H-NMR for Compound **8**

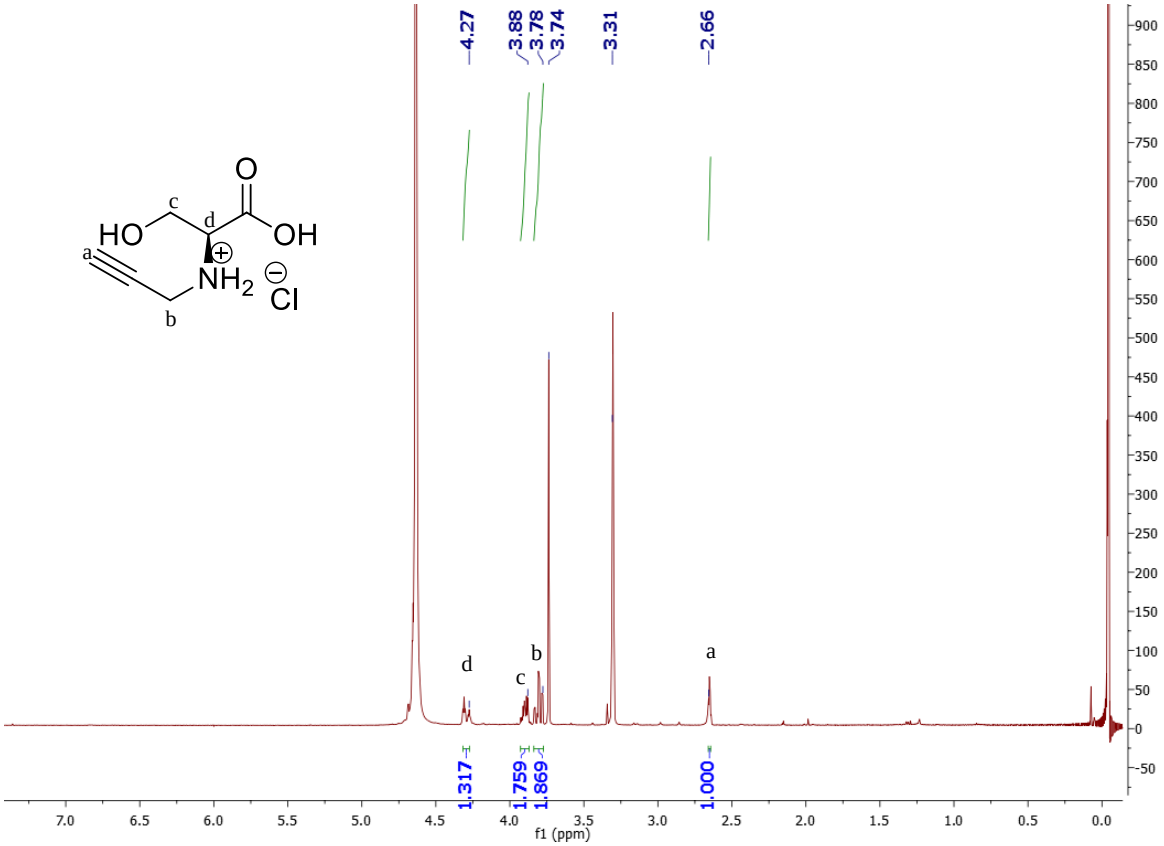

It was initially expected for the ^{1}H-NMR spectrum of Compound **8** to possess four distinct peaks that collectively summed to an integration value of approximately 6. The spectrum matched the expected results. The significant promising piece of the spectrum was the singlet peak located at 2.66 ppm with an integration of 1.00. This peak corresponded to the alkyne hydrogen atom and strongly suggests the correct synthesis of the final compound. In addition, the hydrogen atoms represented by Letters a and d integrated to 1.000 and 1.317 respectively while the hydrogen atoms corresponding to Letters b and c integrated to 1.869 and 1.759 respectively. It was expected for Letters a and d to have integration values equal to approximately 1 and Letters b and c to have integration values equal to approximately 2; the spectrum very closely portrayed the expected integration values.

Figure 14 – ^{13}C-NMR for Compound **8**

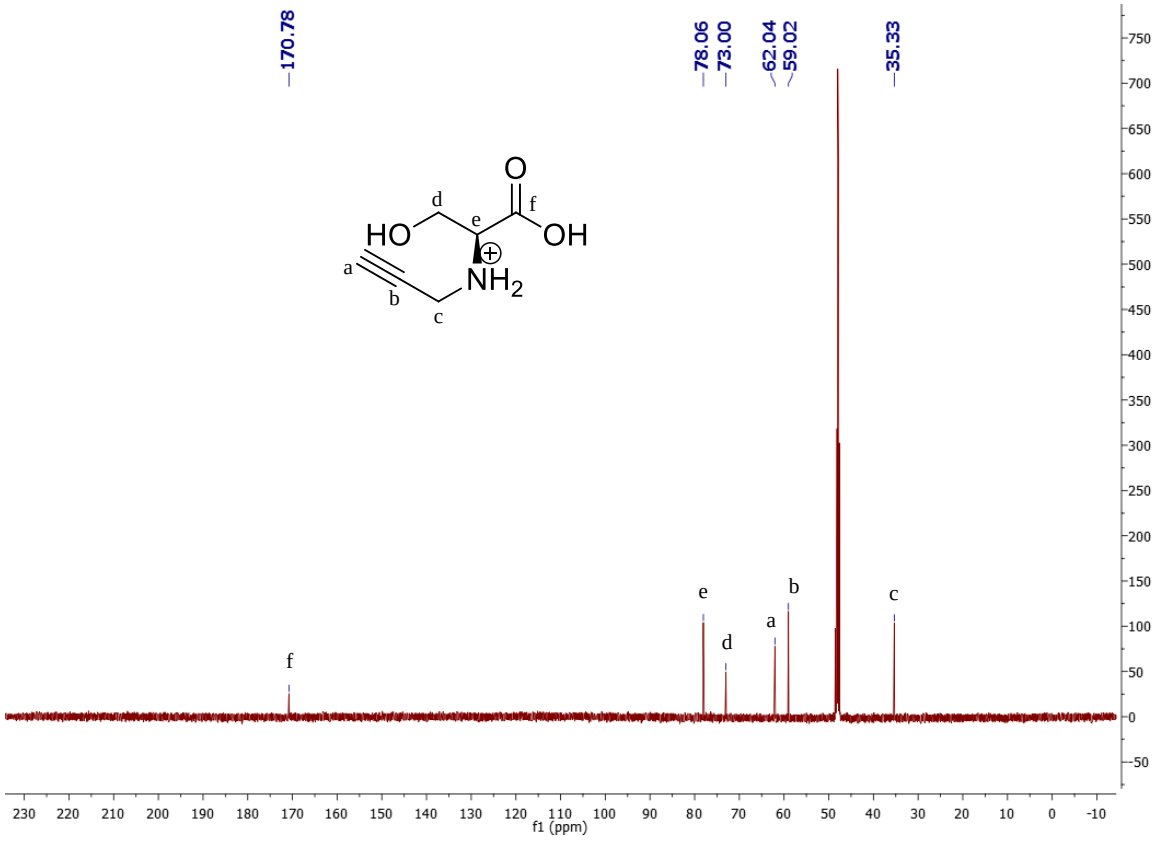

The ^{13}C-NMR data portrayed the expected peak locations for each of the 6 carbon atoms present within Compound **8**. Based on this spectrum, it can be inferred that Compound **8** was synthesized as hoped.

Figure 15 – Mass Spectrometry for Compound **8**

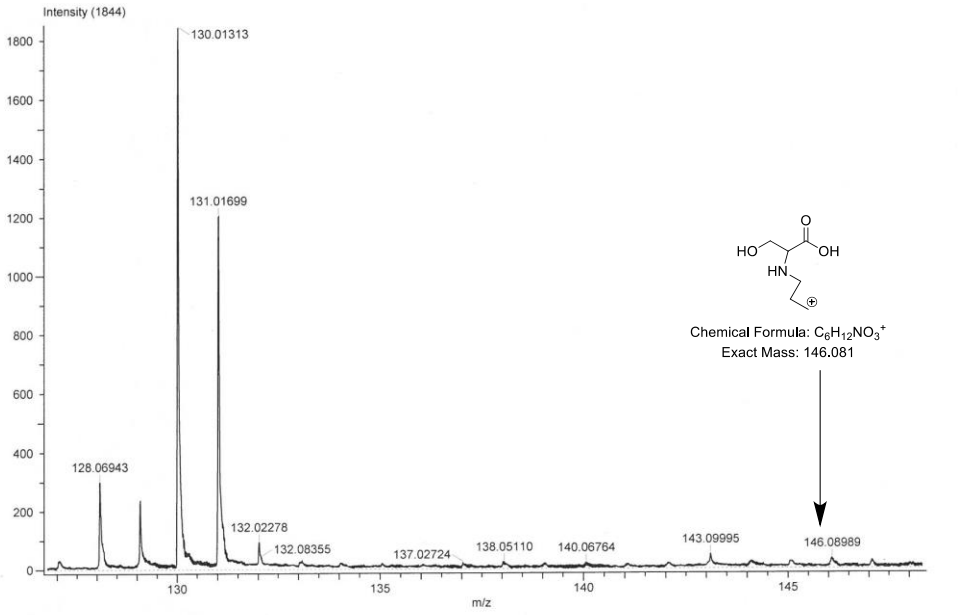

The molecular ion of Compound **8** has an exact weight of 146.081 m/z. Mass spectrometry results shown in Figure 14 portray the molecular ion having a weight of 146.08989 m/z, which represents a percent error value of 0.0000609 % (60.9 ppm) from the exact weight of the molecular ion. Although mass spectrometry cannot confirm the successful formation of Compound **8**, it is strongly suggestive of the correct synthesis of Compound **8**.

Conclusion

Based on the data collected from ^{1}H-NMR, ^{13}C-NMR, and mass spectrometry, it is suggested that the syntheses of (*S*)-3-azido-*N*-(1-carboxy-2-hydroxyethyl)propan-1-aminium (**7**) and (*S*)-*N*-(1-carboxy-2-hydroxyethyl)prop-2-yn-1-aminium (**8**) were successful. While it cannot be entirely confirmed, mass spectrometry and NMR data collected do provide strong evidence of the correct syntheses of **7** and **8**. The NMR data collected for the synthesis of Compound **6**, however, suggests that the final compound likely has more impurities than hoped. Compounds **7** and **8** have already provided very strong results in initial testing of competitive inhibition against the phosphatidylserine synthase Cho1 within *C. albicans* as illustrated in Figures 1 and 2. Compound **6** will soon be tested to determine its degree of competitive inhibition of Cho1 in *C. albicans* as well. In future months, further testing of Compounds **6**, **7**, and **8**, along with new serine analogs that have not yet been synthesized, will hopefully confirm their degree of competitive inhibition of Cho1 within *C. albicans.* The hope is that the syntheses of these compounds will in turn lead to successful inhibition of *C. albicans*, the design of a pharmaceutical drug that can serve as an antifungal therapeutic, and the ultimate diminishing of the harmful effects of Fungal Endocarditis.

References

1. Arnold, Christopher J., Melissa Johnson, Arnold S. Bayer, Suzanne Bradley, Efthymia Giannitsioti, Jose M. Miro, Pilar Tornos, Pierre Tattevin, Jacob Strahilevitz, Denis Spelman, Eugene Athan, Francisco Nacinovich, Claudio Q. Fortes, Cristiane Lamas, Bruno Barsic, Nuria Fernandez – Hidalgo, Patricia Munoz, and Vivian H. Chu. "Candida Infective Endocarditis: An Observational Cohort Study with a Focus on Therapy." *Antimicrobial Agents and Chemotherapy* 59.4 (2015): 2365 – 373. *Web of Science.* Web. 2 Apr. 2016.

2. Chen, Y.L., et al., *Phosphatidylserine synthase and phosphatidylserine decarboxylase are essential for cell wall integrity and virulence in Candida albicans.* Molecular microbiology, 2010. **75**(5): p. 1112-32.

3. Davis, S.E., A. Hopke, S. C. Minkin, A. E. Montedonico, R. T. Wheeler, and T. B. Reynolds. "Masking of (1-3)-Glucan in the Cell Wall of Candida Albicans from Detection by Innate Immune Cells Depend on Phosphatidylserine." *Infection and Immunity* 82.10 (2014): 4405-413. *Web of Science.* Web. 30 Mar. 2016.

4. Donlan, Rodney M. "Biofilm Formation: A Clinically Relevant Microbiological Process." *Clinical Infectious Diseases* 33.8 (2001): 1387 – 92. Web. 20 Mar. 2016.

5. Douglas, L.J. "Candida Biofilms and Their Role in Infection." *Trends in Microbiology* 11.1 (2003): 30 – 36. *Web of Science.* Web. 23 Mar. 2016.

6. Mishra, Nagendra, Tulika Prasad, Neeraj Sharma, Anurag Payasi, Rajendra Prasad, Dwijendra Gupta, and Randhir Singh. "Pathogenicity and Drug Resistance in Candid Albicans and

Other Yeast Species." *Acta Microbiologica Et Immunologica Hungarica* 54.3 (2007): 201 – 35. *Web of Science.* Web. 4 Apr. 2016.

7. O'donnell, Lindsay E., Emma Millhouse, Leighann Sherry, Ryan Kean, Jennifer Malcolm, Christopher J. Nile, and Gordon Ramage. "Polymicrobial Candida Biofilms: Friends and Foe in the Oral Cavity." *FEMS Yeast Research* 15.7 (2015): n. pag. Web. 2 Apr. 2016.

8. Pana, Zoe Dorothea, John Dotis, Elias Losifidis, and Emmanuel Roilides, "Fungal Endocarditis in Neonates." *The Pediatric Infectious Disease Journal* 34.8 (2015): 803 – 08. *Web of Science.* Web. 2 Apr. 2016.

9. Seelig, M.S., P. Goldberg, P.J. Kozinn, and A.R. Berger. "Fungal Endocarditis: Patients at Risk and Their Treatment." *Postgraduate Medical Journal,* U.S. National Library of Medicine. 1979. Web. 30 Mar. 2016.

10. Snider, William D., David M. Simpson, Surl Nielsen, W.M. Jonathan Gold, Craig E. Metroka, and Jerome B. Posner. "Neurological Complications of Acquired Immune Deficiency Syndrome: Analysis of 50 Patients." *Annals of Neurology* 14.4 (1983): 403 – 18. *Web of Science.* Web. 10 Mar. 2016.

11. Sun, L., K. Liao, S. Liang, P. Yu, and D. Wang. "Synergistic Activity of Magnolol with Azoles and Its Possible Antifungal Mechanism against Candida Albicans." *Journal of Applied Microbiology* 118.4 (2015): 826 – 38. *Web of Science.* Web. 4 Apr. 2016.